

involves exchange between the dangling phosphorus atoms and the coordinated terminal phosphorus atoms. In the process the central phosphorus atom remains coordinated.

The stability of the six-membered chelate ring in these complexes limits their manipulation. The four-membered chelate rings formed by 2-(diphenylphosphino)pyridine<sup>25</sup> and bis(diphenylphosphino)methane (dpm)<sup>26,27</sup> are rather easily opened in reactions with other metal ions to give binuclear (particularly heterobinuclear) complexes. In the process a chelated ligand is converted into a bridging ligand. In contrast with dpmp we have not as yet encountered examples of such ring opening. Similarly it is possible to convert chelating dpm into a bridging form by choosing ancillary ligands that prefer to bind in a mutually trans fashion. For example, treatment of Pt(dpm)Cl<sub>2</sub> with sodium cyanide yields *trans*-Pt(CN)<sub>2</sub>(μ-dpm)<sub>2</sub>-*trans*-Pt(CN)<sub>2</sub>.<sup>28</sup> In contrast, Pt(dpmp)(CN)<sub>2</sub> has a chelated structure and *cis* cyanide ligands.

Once formed, these chelate rings can act as additional ligands. The spectroscopic behavior of the polynuclear complexes described

here indicates little if any interaction between the metal centers of these complexes. The spectroscopic data suggest that all of the chelated monomers exist with the boat conformation found crystallographically for Pd(dpmp)Cl<sub>2</sub>. The conversion of the chelating ligand into a bridging ligand appears to be accompanied by a change of ring conformation to the skew-boat conformation 4. This change in ring conformation is interpreted as causing the diminution in the magnitude of *J*(P,P) seen on complexation of the internal phosphorus atom and also causing the increase in the magnitude of *J*(P,H), which results in increased complexity of the upfield methylene resonance in the polynuclear complexes.

**Acknowledgment.** We thank the National Science Foundation (Grant No. CHE8217954) for generous financial support and F. E. Wood, M. W. Renner, and A. J. Fossett for experimental assistance.

**Registry No.** 5, 93862-09-0; 6, 93842-01-4; 7, 86217-37-0; 8, 84751-00-8; 9, 93842-02-5; 10, 93842-03-6; 11, 86217-32-5; 12, 93842-04-7; 13, 93842-05-8; 14, 93842-12-7; 15, 93842-13-8; 16, 93842-06-9; 17, 93921-89-2; 18, 93921-90-5; 19, 93921-91-6; 20, 93842-07-0; 21, 93842-08-1; 22, 93842-09-2; *trans*-PtCl<sub>2</sub>[(μ-dpmp)Mo(CO)<sub>4</sub>]<sub>2</sub>, 93921-92-7; PdCl<sub>2</sub>(μ-dpmp)PdCl<sub>2</sub>(NCCH<sub>3</sub>), 86217-33-6; PdCl<sub>2</sub>[(μ-dpmp)-PdCl<sub>2</sub>]<sub>2</sub>, 93921-93-8; PdCl<sub>2</sub>[(μ-dpmp)Pt(CH<sub>3</sub>)<sub>2</sub>]<sub>2</sub>, 93842-10-5; PdCl<sub>2</sub>[(μ-dpmp)Mo(CO)<sub>4</sub>]<sub>2</sub>, 93842-11-6; (1,5-COD)PdBr<sub>2</sub>, 12145-47-0; (1,5-COD)PtCl<sub>2</sub>, 12080-32-9; Mo(2,5-nor)(CO)<sub>4</sub>, 12146-37-1; [Rh(CO)<sub>2</sub>(μ-Cl)]<sub>2</sub>, 14523-22-9; (1,5-COD)PdCl<sub>2</sub>, 12107-56-1; chromium hexacarbonyl, 13007-92-6; tungsten hexacarbonyl, 14040-11-0.

- (25) Farr, J. P.; Olmstead, M. M.; Wood, F. E.; Balch, A. L. *J. Am. Chem. Soc.* **1983**, *105*, 792.  
 (26) McEwan, D. M.; Pringle, P. G.; Shaw, B. L. *J. Chem. Soc., Chem. Commun.* **1982**, 1240.  
 (27) Hutton, A. T.; Pringle, P. G.; Shaw, B. L. *Organometallics* **1983**, *2*, 1889.  
 (28) Pringle, P. G.; Shaw, B. L. *J. Chem. Soc., Chem. Commun.* **1982**, 956.

Contribution from the Department of Chemistry,  
Brown University, Providence, Rhode Island 02912

## Kinetic Study of the Reaction of Ferric Porphyrin Fluorides and Imidazole

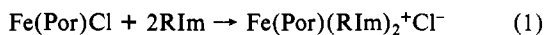
J. G. JONES,\*<sup>1</sup> G. A. TONDREAU, J. O. EDWARDS, and D. A. SWEIGART\*<sup>2</sup>

Received October 8, 1984

A kinetic study is reported for the reaction of Fe(porphyrin)F (porphyrin = dianion of tetraphenylporphyrin (TPP) and protoporphyrin IX dimethyl ester (PIXDME)) with imidazole (HIm) in acetone at 25 °C to give Fe(porphyrin)(HIm)<sub>2</sub><sup>+</sup>F<sup>-</sup>. The reaction rate shows a complex dependence on the HIm concentration, being second order in HIm at low concentrations and progressing to zero order at high concentrations of HIm. With Fe(TPP)F, optical spectra at 25 and -78 °C show the existence of two reaction intermediates. The first intermediate to form is the six-coordinate high-spin Fe(TPP)(HIm)F and the second is Fe(TPP)(HIm)F...HIm, in which an external imidazole is hydrogen bonded to the fluoride. Thus, hydrogen bonding is shown to play a major role in assisting ionization of the fluoride. A comparison to analogous Fe(porphyrin)Cl complexes shows that hydrogen bonding is much more important with the fluoride, as expected for the stronger Brønsted base (F<sup>-</sup> compared to Cl<sup>-</sup>). A complete analysis of the data is provided that yields rate constants as well as equilibrium constants for the formation of both intermediates. The relevance of these reactions to hydrogen bonding to superoxide in oxymetallporphyrins is noted.

### Introduction

The reaction of ferric porphyrin chlorides, Fe(Por)Cl, with imidazoles, RIm, according to eq 1 has been the subject of nu-



merous thermodynamic<sup>3-8</sup> and kinetic<sup>9-12</sup> studies. The initial step

in the reaction is the rapid and reversible conversion of high-spin Fe(Por)Cl to the transient high-spin six-coordinate intermediate Fe(Por)(RIm)Cl, which then dissociates chloride in the rate-determining step before combining with another RIm to give the low-spin product. The mechanistic interest in this reaction has focused on the chloride ionization from the transient intermediate. It has been demonstrated<sup>9-12</sup> that hydrogen bonding to the developing chloride ion can have a major effect on the reaction dynamics. This distal-type hydrogen bonding most clearly manifests itself in the rate laws for unsubstituted imidazole (HIm) and the *N*-methylated analogue (*N*-MeIm). Thus, the reaction

- (1) Permanent address: Department of Chemistry, The New University of Ulster, Coleraine, Northern Ireland.  
 (2) Recipient, NIH Research Career Development Award, 1983-1988.  
 (3) Duclos, J. M. *Bioinorg. Chem.* **1973**, *2*, 263.  
 (4) Coyle, C. L.; Rafson, P. A.; Abbott, E. H. *Inorg. Chem.* **1973**, *12*, 2007.  
 (5) Ciaccio, P. R.; Ellis, J. V.; Munson, M. E.; Kedderis, G. L.; McConville, F. X.; Duclos, J. M. *J. Inorg. Nucl. Chem.* **1976**, *38*, 1885.  
 (6) Walker, F. A.; Lo, M.-W.; Ree, M. T. *J. Am. Chem. Soc.* **1976**, *98*, 5552.  
 (7) Adams, P. A.; Baldwin, D. A.; Hepner, C. E.; Pratt, J. M. *Bioinorg. Chem.* **1978**, *9*, 479.

- (8) Yoshimura, T.; Ozaki, T. *Bull. Chem. Soc. Jpn.* **1979**, *52*, 2268.  
 (9) Budige, D.; Sweigart, D. A. *Inorg. Chim. Acta* **1978**, *28*, L131. Fiske, W.; Sweigart, D. A. *Ibid.* **1979**, *36*, L429.  
 (10) Doeff, M. M.; Sweigart, D. A. *Inorg. Chem.* **1982**, *21*, 3699.  
 (11) Tondreau, G. A.; Sweigart, D. A. *Inorg. Chem.* **1984**, *23*, 1060.  
 (12) Meng, Q.; Tondreau, G. A.; Edwards, J. O.; Sweigart, D. A., submitted for publication.

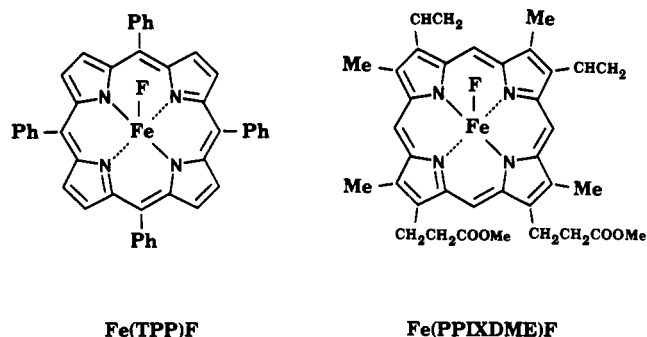
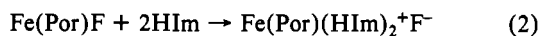


Figure 1. Iron porphyrins used in this study.

with HIm is much faster and follows a fundamentally different rate law compared to that observed with *N*-MeIm. These differences are due to the ability of HIm (but not *N*-MeIm) to assist the chloride ionization via hydrogen bonding. Similar effects are observed with other protic sources, e.g., trifluoroethanol. Even hydrogen bonding by the propionic acid side chains in protoporphyrin IX complexes can significantly influence axial ligand dissociation and association.<sup>12</sup> Studies with cobalt(III) porphyrins indicate that hydrogen bonding to or from an axial ligand has a substantial effect on ligand substitution rates, redox potentials, and <sup>59</sup>Co NMR chemical shifts.<sup>13,14</sup>

If hydrogen bonding to the axial ligand is kinetically and thermodynamically important with the weak Brønsted base chloride, it presumably is even more significant with more basic ligands, the most biologically relevant being superoxide. Hydrogen bonding from the distal histidine to dioxygen is now firmly established for oxyhemoglobin and oxymyoglobin<sup>15,16</sup> and probably stabilizes the polar Fe–O<sub>2</sub> bond without being so strong as to induce HO<sub>2</sub> dissociation (i.e., oxidation). Similarly, hydrogen bonding to dioxygen in model iron and cobalt porphyrins affects thermodynamic stability and the ease of oxidation.<sup>17–20</sup>

In order to extend and verify our earlier work with Fe(Por)Cl complexes, we have investigated reaction 2, in which the porphyrin



is the dianion of tetraphenylporphyrin (TPP) or protoporphyrin IX dimethyl ester (PPIXDME; see Figure 1). Since the axial ligand (fluoride) is a good Brønsted base, it was anticipated that hydrogen-bonding effects would be amplified relative to that observed with chloride. The results are presented herein.

### Experimental Section

All glassware was oven dried prior to use. ACS certified reagent grade acetone was predried for 0.5 h over activated 4-Å molecular sieves, distilled, and dried again for 0.5 h over molecular sieves and filtered through an oven-dried sintered-glass frit. Drying for longer times over molecular sieves does not give a drier solvent because of a condensation reaction that is promoted by sieves. The acetone was generally used within 1 day of purification. The sieves were activated by heating to 200 °C overnight in a vacuum oven. Imidazole (Aldrich) was recrystallized twice from methylene chloride and vacuum dried. Samples further purified by sublimation at 80 °C gave identical experimental results.

Room-temperature optical spectra were recorded on Gilford 250 and Perkin-Elmer 552A spectrophotometers. Spectra at –78 °C were re-

corded on the Perkin-Elmer instrument using a special quartz cell that allows mixing of precooled solutions within the cell and without exposure to the atmosphere.<sup>11</sup> Base line corrections for the low-temperature spectra were made by storing the spectrum of pure solvent (at –78 °C) in the spectrophotometer's memory and subtracting this from the sample spectrum. Kinetic measurements were made at 25 °C (±0.05 °C) with a Dionex 110 stopped-flow instrument. Care was taken to clean and dry all syringes before assembly and to soak the interior of the stopped flow with several changes of dry acetone before use.

**Syntheses.** **Fe(TPP)F.** Initially, this compound was prepared according to a published procedure.<sup>21</sup> However, the reaction of this sample with imidazole followed biphasic kinetics, with the fast step being very similar to that observed with Fe(TPP)Cl. It was concluded that the [Fe(TPP)]<sub>2</sub>O starting material probably contained some Fe(TPP)Cl. More significantly, it was also concluded that the penultimate step of washing the chloroform or methylene chloride solutions of Fe(TPP)F with water caused partial reversion to the  $\mu$ -oxo dimer.

A sample of Fe(TPP)F that gave monophasic kinetics with imidazole was prepared from commercial Fe(TPP)Cl as follows. The principle of the method is to react a nonaqueous solution of Fe(TPP)Cl with an AgF/HF solution, which precipitates AgCl and leaves Fe(TPP)F in the organic phase. This layer is then dried with sodium sulfate, and traces of HF are neutralized with solid NaF. All of these operations must be performed in plastic vessels to avoid contamination by silicofluorides. Fe(TPP)F can then be obtained from the organic layer by evaporation. Further purification can be effected by chromatography on a special column. In a typical preparation, the AgF/HF solution was prepared first. Silver nitrate (3.4 g) was dissolved in 100 mL of water, and a solution containing NaOH (1.0 g) was added. The yellow-brown precipitate of "AgOH" was collected by filtration and washed with water. The damp precipitate was entirely dissolved in 50 mL of 48% HF and the solution kept in a polyethylene bottle. This solution contained ca. 1.25 mol of HF and 0.02 mol of AgF. Fe(TPP)Cl (0.34 g, 0.50 mmol) dissolved in 30 mL of methylene chloride was placed in a polyethylene bottle, and 3 mL of the AgF/HF solution (an excess) was added. On shaking, the red-brown methylene chloride layer changed to green-black. The solution was allowed to stand for 5 min and then was filtered through filter paper. Two filtrations effectively removed the silver chloride precipitate. The organic layer was taken off with a polyethylene Pasteur pipet and dried over anhydrous sodium sulfate and the over anhydrous sodium fluoride powder. The solution was then diluted 50:50 with dried cyclohexane. The mixed solvent was taken off at 40 °C on a rotary evaporator. Lustrous purple crystals appeared as the solvent was removed. These were collected by filtration and oven dried at 80 °C for 1 h. A solution of these crystals in methylene chloride had the same spectrum as the solution from which they were isolated, showing that drying did not lead to decomposition. The spectrum (CH<sub>2</sub>Cl<sub>2</sub>; nm) had bands at 415 (Soret), 482, 545, 615, and 650 with relative strengths 1:0.12:0.057:0.047:0.042. This is similar to spectra reported by Scheidt<sup>21</sup> and Cohen<sup>22</sup> for his "α" form of Fe(TPP)F. The material thus prepared, when purified further by chromatography on the special column described below, gave monophasic kinetics in the experiments herein described.

The problem with column chromatography of Fe(TPP)F on alumina or silica is that almost total transformation to [Fe(TPP)]<sub>2</sub>O occurs. To circumvent this, a special column was made from HF-treated alumina. About 200 g of basic alumina was poured into a 1-L polyethylene bottle with stopper, and 48% HF was added. The alumina became extremely hot, and more HF was added until a stiff pastry gel resulted. Excess HF solution was decanted off, and the gel was dried by washing with acetone. The gel was further dried on filter paper in an oven at 80 °C overnight, after which the gel was crushed to a fine powder and heated again for 1 h at 80 °C. To a dry column of the powder was added a CH<sub>2</sub>Cl<sub>2</sub> solution of Fe(TPP)F. Separation occurred into a black band on top of the column, a brown band, and a pink forerun. The forerun gave a porphyrin-like optical spectrum, with a Soret band at 415 nm and additional bands at 390 (sh), 470 (sh), 500 (sh), 540, and 575 (sh) nm. The main-product solution was brown-yellow and had a spectrum like that reported<sup>21</sup> for Fe(TPP)F, but with better separation between maxima and minima. This solution was evaporated to one-fourth of its original volume and the product precipitated with pentane or cyclohexane and collected by centrifugation. Anal. Calcd: C, 76.86; H, 4.10; N, 8.15; Fe, 8.12; F, 2.76. Found: C, 75.78; H, 4.23; N, 7.87; Fe, 7.83; F, 2.89. After this, the column was stripped with 80:20 acetone/methylene chloride. This stripped fraction consisted mainly of Fe(TPP)F and was worked up as

(13) Doeff, M. M.; Sweigart, D. A.; O'Brien, P. *Inorg. Chem.* **1983**, *22*, 851.

(14) Edwards, J. O.; Hagen, K.; Jones, J. G.; Mahmood, A.; O'Brien, P.; Schwab, C.; Sweigart, D. A., unpublished results.

(15) Phillips, S. E. V.; Schoenborn, B. P. *Nature (London)* **1981**, *292*, 81.

(16) Shaanan, B. *Nature (London)* **1982**, *296*, 683.

(17) Mometeau, M.; Lavalette, D. *J. Chem. Soc., Chem. Commun.* **1982**, *341*. Mispelter, J.; Mometeau, M.; Lavalette, D.; Lhoste, J.-M. *J. Am. Chem. Soc.* **1983**, *105*, 5165.

(18) Dokuzovic, Z.; Ahmeti, X.; Pavlovic, D.; Murati, L.; Asperger, S. *Inorg. Chem.* **1982**, *21*, 1576. Stynes, D. V.; Stynes, H. C.; Ibers, J. A.; James, B. R. *J. Am. Chem. Soc.* **1973**, *95*, 1142.

(19) Jameson, G. B.; Drago, R. S., submitted for publication.

(20) Mims, M. P.; Porras, A. G.; Olson, J. S.; Noble, R. W.; Peterson, J. A. *J. Biol. Chem.* **1983**, *258*, 14219.

(21) Anzai, K.; Hatano, K.; Lee, Y. J.; Scheidt, W. R. *Inorg. Chem.* **1981**, *20*, 2337.

(22) Cohen, I. A.; Summerville, D. A.; Su, S. R. *J. Am. Chem. Soc.* **1976**, *98*, 5813.

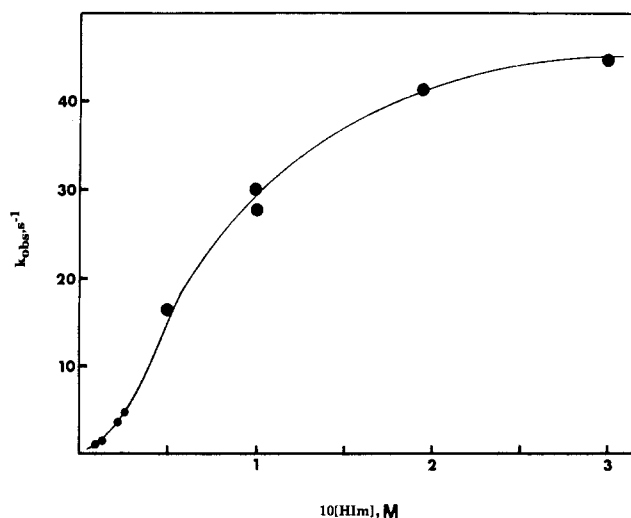


**Figure 2.** Rate constants in acetone at 25 °C for  $\text{Fe}(\text{TPP})\text{F} + 2\text{HIm} \rightarrow \text{Fe}(\text{TPP})(\text{HIm})_2^+\text{F}^-$ .

described above. Both samples gave identical results in kinetic experiments.

**Fe(PPIXDME)F.** The method of preparation involved the esterification of hemin chloride to yield  $[\text{Fe}(\text{PPIXDME})_2\text{O}]^{2+}$  and then treating this with HF. In a typical preparation, 0.33 g of the  $\mu$ -oxo dimer in 150 mL of chloroform was reacted with 70 mL of 5% HF for 5 min. The chloroform layer was washed with 100 mL of water and dried over magnesium sulfate. Solvent evaporation gave a 75% yield of product. The material made this way had been stored for 1 year in a freezer and before use in kinetics experiments was dissolved in benzene, shaken briefly with 48% HF, and then dried over NaF (which absorbs HF) and anhydrous sodium sulfate. The dried solution was reduced in volume until precipitation occurred, and the product was collected by centrifugation and dried for 1 h under high vacuum. The product was analyzed by dissolving a sample in acetone and adding excess imidazole to generate  $\text{Fe}(\text{PPIXDME})(\text{HIm})_2^+\text{F}^-$ . The optical spectrum of this solution was virtually identical in both spectral profile and extinction coefficients with that for the known<sup>8,12</sup>  $\text{Fe}(\text{PPIXDME})(\text{HIm})_2^+\text{Cl}^-$ . The optical spectrum of  $\text{Fe}(\text{PPIXDME})\text{F}$  in acetone has bands at 400, 485, 515 (sh), and 601 nm.  $\text{Fe}(\text{PPIXDME})\text{F}$  and the previously reported<sup>24</sup> iron deuteroporphyrin IX dimethyl ester fluoride have similar spectral profiles, with the protohemin complex having  $\lambda_{\text{max}}$  values at slightly longer wavelengths (by ca. 10 nm), as expected.<sup>23</sup> Solid samples and solutions of  $\text{Fe}(\text{PPIXDME})\text{F}$  were prepared under subdued light and then wrapped in aluminum foil to prevent photooxidation.

## Results and Discussion

**Reactions. Fe(TPP)F with Imidazole.**  $\text{Fe}(\text{TPP})\text{F}$  reacts rapidly with HIm in acetone to give  $\text{Fe}(\text{TPP})(\text{HIm})_2^+\text{F}^-$ , which has an optical spectrum almost identical with that for  $\text{Fe}(\text{TPP})(\text{HIm})_2^+\text{Cl}^-$ . The equilibrium constant ( $\beta_2$ ) for reaction 2 (Por = TPP) was determined in acetone at 25 °C by a spectrophotometric titration at  $\lambda = 640$  nm of  $\text{Fe}(\text{TPP})\text{F}$  with various concentrations of HIm and plotting the results according to eq 3, in which  $A_0$  and  $A_\infty$  refer to the absorbance of  $\text{Fe}(\text{TPP})\text{F}$  and  $\text{Fe}(\text{TPP})(\text{HIm})_2^+\text{F}^-$ , respectively. Above  $[\text{HIm}] = 0.010$  M, the plot was linear with a slope of 2.0 and gave  $\beta_2 = 1.7 \times 10^4 \text{ M}^{-2}$ .

$$\log [(A_0 - A)/(A - A_\infty)] = 2 \log [\text{HIm}] + \log \beta_2 \quad (3)$$

Kinetic studies at 25 °C in acetone were done under pseudo-first-order conditions with the HIm concentration in at least a 100-fold excess over that of  $\text{Fe}(\text{TPP})\text{F}$ . Standard plots of  $\ln(A - A_\infty)$  vs. time were linear over 3–4 half-lives. The dependence of the first-order rate constant ( $k_{\text{obsd}}$ ) on HIm concentration is shown in Figure 2. Most of the experiments were done at  $\lambda = 490$  nm, where a decrease in absorbance occurs. The rate constants were independent of the porphyrin concentration and the wave-

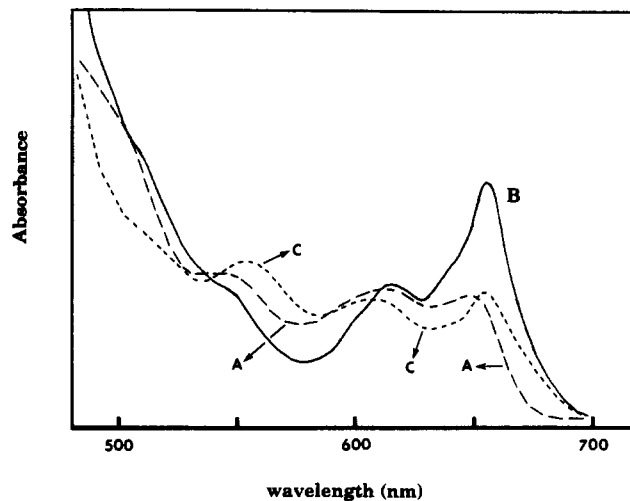


**Figure 3.** Optical spectra in acetone at -78 °C: (A)  $\text{Fe}(\text{TPP})\text{F}$ ; (B)  $\text{Fe}(\text{TPP})\text{F}$  plus 0.0040 M HIm to give an intermediate; (C) solution B warmed to 25 °C and recooled to -78 °C to give product mixture.

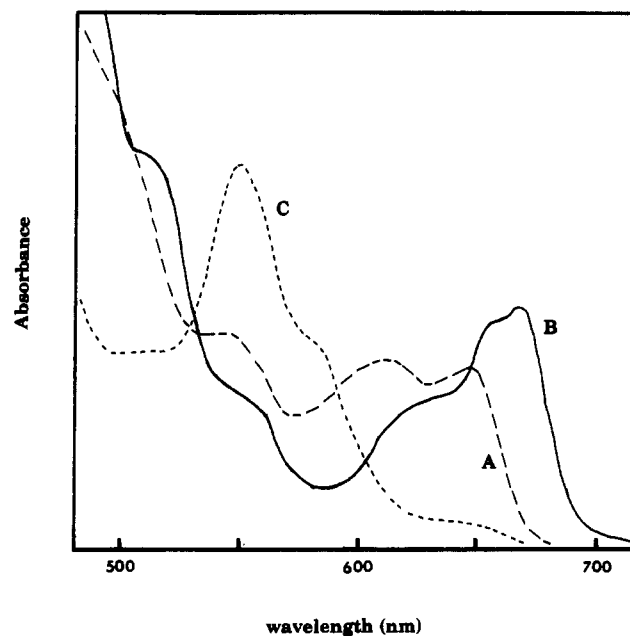


**Figure 4.** Optical spectra in acetone at -78 °C: (A)  $\text{Fe}(\text{TPP})\text{F}$ ; (B)  $\text{Fe}(\text{TPP})\text{F}$  plus 0.038 M HIm to give intermediate species; (C) solution B warmed to 25 °C and recooled to -78 °C to give  $\text{Fe}(\text{TPP})(\text{HIm})_2^+\text{F}^-$ .

length ( $\lambda = 450, 490, 550, 630$  nm). However, the absorbance change expected from static spectra did not always match that observed during the kinetic runs. For example, at 450 nm a decrease in absorbance was observed, although spectra show that  $A_\infty > A_0$ . This obviously suggests the presence of reaction intermediate(s) at significant concentrations, as was observed with  $\text{Fe}(\text{TPP})\text{Cl}$ .<sup>9-12</sup> To investigate this matter further, optical spectra were recorded at -78 °C, at which temperature it was hoped the intermediate species would be metastable. With  $[\text{HIm}] = 0.004$  M there was clear evidence (Figure 3) for an intermediate being formed, with a spectral maximum at 655 nm that is not present in  $\text{Fe}(\text{TPP})\text{F}$  at -78 °C or in the product mixture formed by warming and then recooling the solution. Spectra using  $[\text{HIm}] = 0.038$  M showed an intermediate similar to the one formed at  $[\text{HIm}] = 0.004$  M, but with an additional maximum at 667 nm and other areas of enhanced absorbance (e.g., 635 nm; Figure 4). The product spectrum with  $[\text{HIm}] = 0.038$  M is simply that of  $\text{Fe}(\text{TPP})(\text{HIm})_2^+\text{F}^-$ . Thus, there is evidence for the existence of two intermediates at -78 °C. It is important to realize, however, that the intermediates probably form exothermally, meaning that HIm concentrations most likely must be considerably higher to form the respective intermediates at room temperature.

(23) O'Keeffe, D. H.; Barlow, C. H.; Smythe, G. A.; Fuchsman, W. H.; Moss, T. H.; Lilienthal, H. R.; Caughey, W. S. *Bioinorg. Chem.* **1975**, *5*, 125.

(24) Momenteau, M.; Mispelter, J.; Lexa, D. *Biochim. Biophys. Acta* **1973**, *320*, 652.

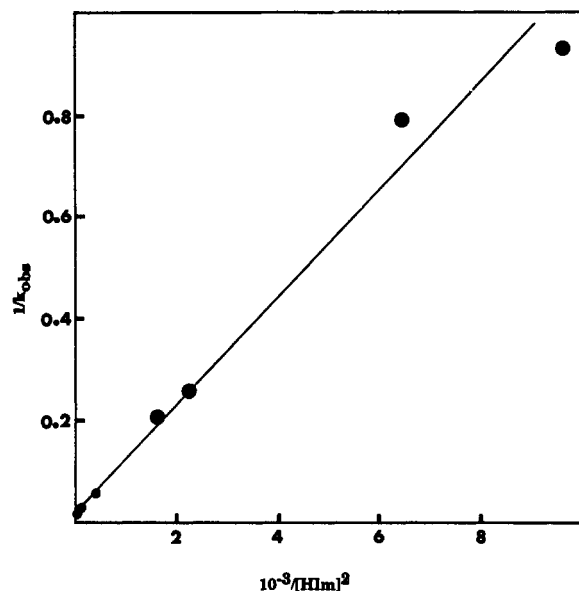


Figure 5. Reciprocal plot of the rate data in Figure 2.

An attempt was made to determine the formation constant for the intermediate(s) at 25 °C by measuring the dependence of the observed absorbance change ( $\Delta A_{\text{obsd}}$ ) on the HIm concentration. Using the stopped flow,  $\Delta A_{\text{obsd}}$ ,  $A_0$ , and  $A_\infty$  were recorded. If no intermediate is formed,  $\Delta A_{\text{obsd}}$  should equal  $A_\infty - A_0$ . However, if Fe(TPP)F is wholly or partially converted to an intermediate before the rate-determining step, then the apparent initial absorbance ( $A_\infty - \Delta A_{\text{obsd}}$ ) will not equal  $A_0$ . This was the case at  $\lambda = 655$  and 670 nm. A plot of  $(A_\infty - \Delta A_{\text{obsd}})$  vs.  $(A_\infty - A_0 - \Delta A_{\text{obsd}})/[\text{HIm}]$  was linear, meaning that under these conditions only the first intermediate formed.<sup>10</sup> From the slope of the plot, the formation constant ( $K_1$ ) was calculated to be  $20 \pm 5 \text{ M}^{-1}$ . It is highly probable that this intermediate is the six-coordinate complex Fe(TPP)(HIm)F in which HIm is coordinated trans to the fluoride. The analogous Fe(TPP)(HIm)Cl complex is known<sup>11</sup> to have a formation constant of ca.  $13 \text{ M}^{-1}$ .

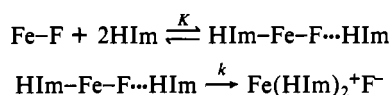
The  $k_{\text{obsd}}$  vs.  $[\text{HIm}]$  plot in Figure 2 suggests a rather complex mechanism for which the order in HIm varies from near 2 at low  $[\text{HIm}]$  to 0 at high  $[\text{HIm}]$ . By contrast, the reaction of Fe(TPP)Cl is simply second order in HIm over the accessible range of  $[\text{HIm}]$  (0.005–0.08 M).<sup>11</sup> The rate law for Fe(TPP)F fits expression 4

$$k_{\text{obsd}} = \frac{kK[\text{HIm}]^2}{1 + K[\text{HIm}]^2} \quad (4)$$

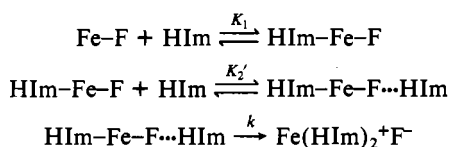
$$k_{\text{obsd}} = \frac{kK_1K_2'[\text{HIm}]^2}{1 + K_1[\text{HIm}] + K_1K_2'[\text{HIm}]^2} \quad (5)$$

as shown by plotting  $1/k_{\text{obsd}}$  vs.  $1/[\text{HIm}]^2$  (Figure 5). The plot in Figure 5 gives  $k = 45 \pm 5 \text{ s}^{-1}$  and  $K = 210 \pm 30 \text{ M}^{-2}$ . Two mechanisms considered reasonable in view of the intermediates discussed above are given in Schemes I and II (Fe–F denotes

#### Scheme I



#### Scheme II



Fe(TPP)F). For Scheme I the rate law is given by eq 4, and for Scheme II the rate constant is given by eq 5. Of course, Scheme II is simply a more elaborate version of Scheme I. In principle,

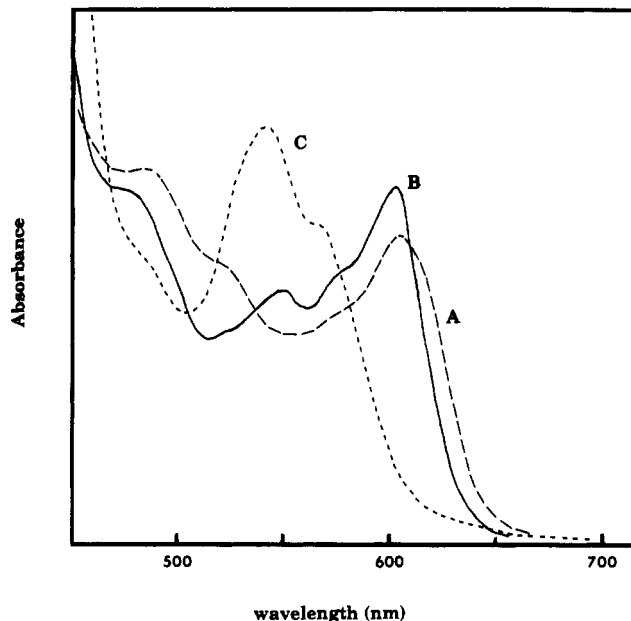


Figure 6. Optical spectra in acetone at  $-78$  °C: (A) Fe(PPIXDME)F; (B) Fe(PPIXDME)F plus 0.074 M HIm to give intermediate species; (C) solution B warmed to 25 °C and recooled to  $-78$  °C to give Fe(PPIXDME)(HIm) $_2^+\text{F}^-$ .

an appropriate reciprocal plot can distinguish between these mechanisms. Thus, the linear plot in Figure 5 fits eq 4 and implicates Scheme I since eq 5 should not give a linear fit of  $1/k_{\text{obsd}}$  vs.  $1/[\text{HIm}]^2$ . In practice, however, the fit would be fairly good to eq 5 for reasonable values of the rate constants, and so the kinetic data alone do not justify a choice. However, since there is evidence for two intermediates from the  $-78$  °C optical spectra, and since the formation constant of the first of these was obtained from room-temperature data, it seems appropriate to analyze the results in terms of Scheme II. The composite equilibrium constant  $K$ , obtained from Figure 5, is then identified as  $K_1K_2'$  ( $210 \pm 30 \text{ M}^{-2}$ ). Since  $K_1$  could be estimated as  $20 \pm 5 \text{ M}^{-1}$ , it follows that  $K_2' = 10 \pm 4 \text{ M}^{-1}$ .

The most reasonable structure for the second intermediate has HIm hydrogen bonded to fluoride (see Scheme II). The rather strong Brønsted basicity of fluoride makes this a reasonable possibility and accounts for the failure to detect a similar intermediate in the reaction of Fe(TPP)Cl.<sup>11</sup>

**Fe(PPIXDME)F with Imidazole.** Kinetic experiments for this reaction were performed similarly to those with Fe(TPP)F, and the kinetics were found to be biphasic. Attempted further purification of Fe(PPIXDME)F by using the HF-treated alumina column was not successful because the complex stuck strongly to the top of the column and could not be eluted. By chance, it was discovered that the biphasic nature of the reaction depended on the porphyrin concentration. At low concentrations the faster of the two steps accounted for almost all of the absorbance change, while at higher concentrations the slower step was dominant. This suggests that the faster step is due to monomeric porphyrin reacting and that the slower step derives from dimeric species. Such dimerization apparently does not occur with Fe(TPP)F, perhaps due to the steric bulk of the *meso*-phenyl groups. Accordingly, with Fe(PPIXDME)F, attention was focused on the faster step and a low porphyrin concentration was used (ca.  $5 \times 10^{-6} \text{ M}$ ) so that the slower step was minimized. The wavelength used was 380 nm. Optical spectra at  $-78$  °C again indicated an intermediate, but evidence could not be obtained for two separate intermediates as seen with Fe(TPP)F. Figure 6 shows the spectra. The intermediate has a maximum at  $\lambda = 603 \text{ nm}$ , suggesting that it is high spin<sup>25</sup> as would be expected.<sup>9-12</sup> The final product (obtained after warming and recooling) has a spectrum virtually

(25) Smith, D. W.; Williams, R. J. P. *Struct. Bonding (Berlin)* 1970, 7, 1.

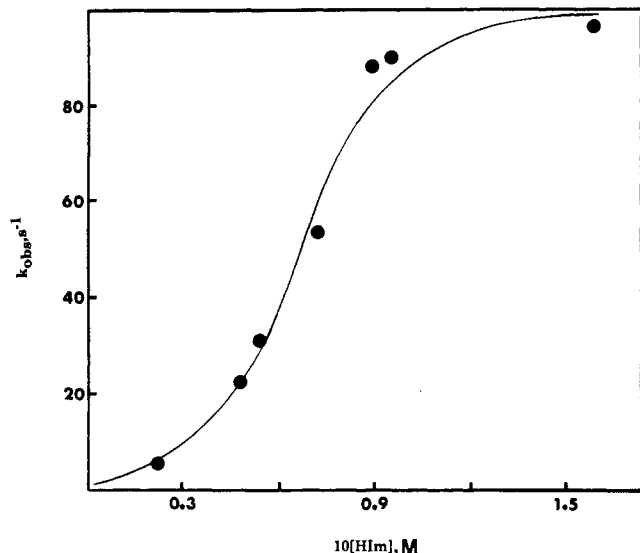


Figure 7. Rate constants in acetone at 25 °C for Fe(PPIXDME)F + 2HIm  $\rightarrow$  Fe(PPIXDME)(HIm)<sub>2</sub><sup>+</sup>F<sup>-</sup>.

identical with that for Fe(PPIXDME)(RIm)<sub>2</sub><sup>+</sup>Cl<sup>-</sup>.<sup>12</sup>

The variation of  $k_{\text{obs}}$  with [HIm] is shown in Figure 7. The results are similar to that seen with Fe(TPP)F, and treatment of the data in the same manner gave (see Scheme I)  $kK = 12000 \pm 3000 \text{ s}^{-1} \text{ M}^{-2}$ ,  $k = 100 \pm 30 \text{ s}^{-1}$ , and  $K = 120 \pm 50 \text{ M}^{-2}$ .

**Comparison of the Reactions of Fe(Por)F and Fe(Por)Cl.** As stated in the Introduction, one purpose of this study was to determine whether the hydrogen-bonding effects seen with Fe(Por)Cl are amplified with Fe(Por)F. The most striking difference between these metalloporphyrins is the rate law. Thus, Fe(Por)Cl reacts with HIm according to a simple rate law second order in HIm, while the order approaches zero in HIm with Fe(Por)F. Nevertheless, there are significant similarities between the two porphyrins. At low HIm concentrations, both are second order in HIm, showing that two molecules of HIm are involved in the transition state. Furthermore, both form a six-coordinate high-spin intermediate, Fe(Por)(HIm)X, with similar formation constants ( $K_1$ ). Table I lists the various constants that merit comparison. The most important difference appears in  $K_2'$ . The chloride in Fe(Por)(HIm)Cl does not hydrogen bond to external HIm to a detectable extent in the ground state, and so the observed acceleration of chloride ionization in the presence of HIm (e.g., compared to *N*-MeIm) reflects hydrogen bonding to the developing chloride ion in the transition state. With Fe(Por)(HIm)F, however, hydrogen bonding to the fluoride occurs in the ground state and is responsible for the observed saturation kinetics. The

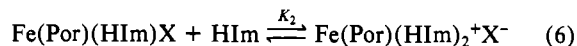
Table I. Comparison of Rate and Equilibrium Constants for the Reaction of Fe(Por)F and Fe(Por)Cl with Imidazole<sup>a</sup>

complex	$10^4 \beta_2$ , M <sup>-2</sup>	$kK$ or $\bar{k}\bar{K}$ , <sup>b</sup> M <sup>-2</sup> s <sup>-1</sup>	$K_1$ , M <sup>-1</sup>	$K_2'$ , M <sup>-1</sup>	$K_2$ , <sup>c</sup> M <sup>-1</sup>	$kK_2'$ , <sup>d</sup> M <sup>-1</sup> s <sup>-1</sup>
Fe(TPP)Cl	16	5900	13	v small	12000	450
Fe(TPP)F	1.7	9500	20	10	800	450
Fe(PPIXDME)Cl	7	5200	9		8000	580
Fe(PPIXDME)F		12000				

<sup>a</sup> All data are at 25 °C in acetone; see Schemes I and II for the meaning of the symbols. <sup>b</sup> Equivalent to initial slope in plot of  $k_{\text{obs}}$  vs. [HIm]. The quantity  $kK$  refers to Fe(Por)F; the equivalent quantity for Fe(Por)Cl is  $\bar{k}\bar{K}$ , where  $\bar{K}$  is the same as  $K_1$  and  $\bar{k}$  is the second-order rate constant for the reaction Fe(Por)(HIm)Cl + HIm  $\rightarrow$  Fe(Por)(HIm)<sub>2</sub><sup>+</sup>Cl<sup>-</sup>;  $\bar{k}$  is also the same as  $kK_2'$ . <sup>c</sup> Computed as  $\beta_2/K_1$ . <sup>d</sup> For Fe(Por)Cl this is the same as  $\bar{k}$ .

quantity  $kK_2'$  measures the rate of conversion of Fe(Por)(HIm)X to product, Fe(Por)(HIm)<sub>2</sub><sup>+</sup>X<sup>-</sup>. This quantity is the same for X = Cl<sup>-</sup> and F<sup>-</sup>, meaning that  $k$  is much larger for X = Cl<sup>-</sup>. Most likely this is due to a weaker Fe-X bond for X = Cl<sup>-</sup>. For the same reason the quantities  $kK$  and  $\bar{k}\bar{K}$  are similar for both halides.

The overall equilibrium constant ( $\beta_2$ ) is significantly greater with X = Cl<sup>-</sup>, and this is largely reflected in  $K_2$ , which refers to eq 6. The much larger  $K_2$  value for X = Cl<sup>-</sup> again is no doubt due to a weaker Fe-Cl bond compared to Fe-F.



In conclusion we observe that Fe(Por)Cl and Fe(Por)F react with HIm according to the same mechanism in which hydrogen bonding to the departing halide is featured. The role played by hydrogen bonding is greatly amplified with the fluoride complex. This effect brings the overall reactivity of Fe(Por)F up to that of Fe(Por)Cl and results in saturation kinetics with the former. On the basis of these results, it seems likely that hydrogen bonding to superoxide in Fe(Por)(base)O<sub>2</sub> complexes should have significant thermodynamic and kinetic consequences. We plan to investigate such effects with oxycobalt and iron porphyrins. Also in progress is a study of the reaction of Fe(Por)N<sub>3</sub> and imidazole. This system differs significantly from the halide analogues in that the Fe(Por)(HIm)N<sub>3</sub> intermediates are low spin and have large  $K_1$  values.

**Acknowledgment.** This work was supported by grants from the National Institutes of Health (Grant Nos. AM 30145 and AM 01151). J.G.J. thanks Brown University for a visiting professorship and the New University of Ulster for a study leave.

**Registry No.** HIm, 288-32-4; Fe(TPP)F, 55428-47-2; Fe(PPIXDME)F, 14724-62-0.